GEOLOGY | THE GEOLOGICAL SOCIETY OF AMERICA®

https://doi.org/10.1130/G47400.1

Manuscript received 21 October 2019
Revised manuscript received 5 March 2020
Manuscript accepted 14 March 2020

Published online 29 April 2020

The role of the westerlies and orography in Asian hydroclimate since the late Oligocene

Xin Wang[1]*, Barbara Carrapa[2], Yuchen Sun[3], David L. Dettman[2], James B. Chapman[4], Jeremy K. Caves Rugenstein[5], Mark T. Clementz[4], Peter G. DeCelles[2], Mi Wang[1], Jie Chen[1], Jay Quade[2], Fei Wang[1], Zaijun Li[1], Ilhomjon Oimuhammadzoda[6], Mustafo Gadoev[6], Gerrit Lohmann[3], Xu Zhang[1,3] and Fahu Chen[1,7]*

[1]Key Laboratory of Western China's Environmental Systems (Ministry of Education), College of Earth and Environmental Sciences, Center for Pan-third Pole Environment (Pan-TPE), Lanzhou University, Lanzhou 730000, China
[2]Department of Geosciences, University of Arizona, Tucson, Arizona 85721, USA
[3]Alfred Wegener Institute, Helmholtz Centre for Polar and Marine Research, Bremerhaven D-27570, Germany
[4]Department of Geology and Geophysics, University of Wyoming, Laramie, Wyoming 82071, USA
[5]Department of Earth Sciences, ETH Zürich, Zürich 8092, Switzerland
[6]Institute of Geology, Earthquake Engineering and Seismology of the Academy of Sciences, Dushanbe 734063, Tajikistan
[7]Key Laboratory of Alpine Ecology, Center for Excellence in Tibetan Plateau Earth Sciences and Institute of Tibetan Plateau Research, Chinese Academy of Sciences (CAS), Beijing 100101, China

ABSTRACT

Interactions between midlatitude westerlies and the Pamir–Tian Shan mountains significantly impact hydroclimate patterns in Central Asia today, and they played an important role in driving Asian aridification during the Cenozoic. We show that distinct west-east hydroclimate differences were established over Central Asia during the late Oligocene (ca. 25 Ma), as recorded by stable oxygen isotopic values of soil carbonates. Our climate simulations show that these differences are present when relief of the Pamir–Tian Shan is higher than 75% of modern elevation (~3000 m). Integrated with geological evidence, we suggest that a significant portion of the Pamir–Tian Shan orogen had reached elevations of ~3 km and acted as a moisture barrier for the westerlies since ca. 25 Ma.

INTRODUCTION

Central Asia constitutes the largest extratropical arid zone on Earth. However, during the early Cenozoic, most of this region was warmer and wetter than present day and periodically occupied by the Paratethys, an epicontinental seaway that stretched from the Atlantic Ocean to the Tarim Basin. Numerous studies suggest a complex aridification history of Central Asia during the Cenozoic, but the mechanisms responsible for this drying trend remain controversial (An, 2014).

Asian aridification has been related to the retreat of the Paratethys (Ramstein et al., 1997), the uplift of the Tibetan Plateau (Liu et al., 2015), and/or global cooling (Lu et al., 2010). Recent work suggests that interactions between the westerlies and the Pamir–Tian Shan played an important role in controlling hydroclimate changes over Central Asia (Caves et al., 2015; Heermance et al., 2018). However, the timing when this topographic-atmospheric framework was established remains poorly constrained.

Precipitation in Central Asia concentrates in boreal winter seasons (Fig. S1in the Supplemental Material[1]), and its variability is mainly influenced by the location and intensity of the westerlies (Chen et al., 2019). Blocked by the Pamir and Tian Shan, the modern westerlies are split into two branches, with precipitation higher on the western flanks (windward) of the Pamir–Tian Shan and significantly lower on the eastern side (leeward; Fig. 1B). Seasonally, the regions west of these mountains have winter-spring precipitation maxima, whereas regions to the east have summer precipitation maxima (Fig. S1). These distinct west-east hydroclimate differences are closely related to the orographic barrier, which intercepts moisture in the westerlies, blocks winter precipitation, and enhances subsidence over the leeward side (Baldwin and Vecchi, 2016).

The Pamir formed as a result of accretion of allochthonous terranes to Eurasia during the Mesozoic and subsequent significant uplift during the Cenozoic (Chapman et al., 2019). The Tian Shan is a Paleozoic orogen that was reactivated during the late Cenozoic (Sobel and Dumitru, 1997). The Tajik and Tarim Basins (Fig. 1C) are foreland basins related to the uplift of the Pamir that developed by no later than ca. 40 Ma (Carrapa et al., 2015; Chapman et al., 2019), as supported by geochemical and geological data from the Tarim Basin indicating high elevations in the eastern Pamir by no later than Oligocene time (Bershaw et al., 2012). Cenozoic sedimentary sequences in these basins (Fig. S2) provide ideal archives for understanding paleoclimate changes in Central Asia. Although a connection between the two basins through what is now the Alai valley existed throughout the Cenozoic, the growth of the Pamir (Wang et al., 2019; Blayney et al., 2019; Chapman et al., 2019) and of the western Tian Shan (Bande et al., 2017; Jepson et al., 2018) as early as the Oligocene suggests

*E-mails: xinw@lzu.edu.cn; fhchen@itpcas.ac.cn.

[1]Supplemental Material. Detailed description of sample analyses, geological setting, model simulation, and the data presented in the paper. Please visit https://doi.org/10.1130/GEOL.26213S.12114426 to access the supplemental material, and contact editing@geosociety.org with any questions.

CITATION: Wang, X., et al., 2020, The role of the westerlies and orography in Asian hydroclimate since the late Oligocene: Geology, v. 48, p. 728–732, https://doi.org/10.1130/G47400.1

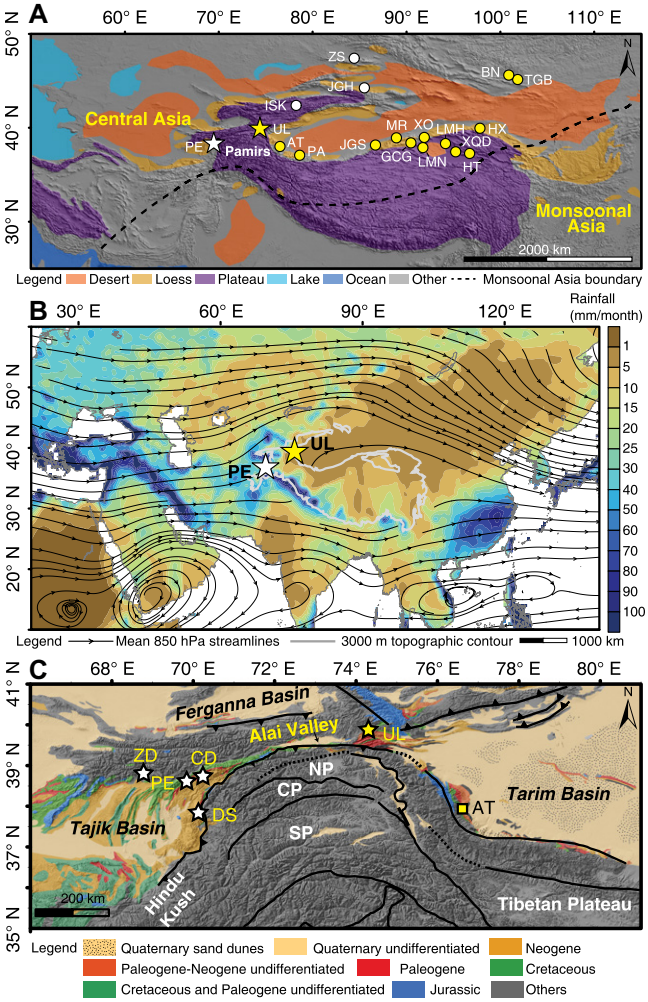

Figure 1. Maps showing location and geological setting of the study area in Central Asia. (A) Schematic map showing loess and desert distribution in midlatitude Asia. (B) December-January-February rainfall based on National Centers for Atmospheric Prediction–National Center for Atmospheric Research (NCEP/NCAR) reanalysis data during 1971–2000 (Kalnay et al., 1996). (C) Simplified geologic map of study area (Carrapa et al., 2015). Star indicates working sections (this study); circle indicates comparison sections. Abbreviations: PE—Peshtova; ZD—Zidi; DS—Dashtijum; UL—Ulugqat; AT—Aertashi; PA—Puska; MR—Miran River; JGS—Janggalsay; XO—Xorkol; HX—Hexi Corridor; GCG—Ganchaigou; LLH—Lulehe; LMH—Lake Mahai; LMN—Laomangnai; XQD—Xiao Qaidam (Kent-Corson et al., 2009); ISK—Issyk Kul (Macaulay et al., 2016); ZS—Zaysan (Caves et al., 2017); UL—Ulugqat (Wang et al., 2014); JGH—Jingouhe (Charreau et al., 2012); HT—Huaitoutala (Zhuang et al., 2011); BN—Biger Noor; TGB—Taatsin Gol (Caves et al., 2014); NP—northern Pamir; CP—central Pamir; SP—southern Pamir.

that the westerly atmospheric flow was disrupted by high topography in the region beginning in the early Cenozoic.

METHODS

We applied stable oxygen isotope geochemistry to well-dated Eocene–Miocene sedimentary rocks from the Tajik Basin and to Eocene sedimentary rocks from the western Tarim Basin (Fig. 2). We then integrated our results with published stable oxygen isotopic data from adjacent regions (Kent-Corson et al., 2009; Zhuang et al., 2011; Charreau et al., 2012; Caves et al., 2014, 2017; Macaulay et al., 2016) to evaluate regional precipitation changes across topography. We also conducted elemental geochemical and clay mineralogical analyses of siltstone samples (modal grain size: 5–63 µm) from the Tajik Basin as a proxy for weathering in the basin and its catchment. Finally, we performed climate simulations, using the Atmosphere General Circulation Model (Stepanek and Lohmann, 2012), to evaluate the impact of topographic changes in the Pamir and Tian Shan on Central Asia climate. Detailed methods are described in the Supplemental Material.

RESULTS

The $\delta^{18}O$ values (relative to Vienna Peedee belemnite [VPDB]) of sandstone and mudstone cements from Cenozoic nonmarine sedimentary rocks (Fig. S3) in the Tajik Basin ranged from −7.51‰ to −13.48‰, with an average value of −10.46‰ (Fig. 2; Table S1). The $\delta^{18}O_{cc}$ (cc—carbonate cements) values were highest (~−8.67‰) in the Paleocene to Middle Eocene continental deposits. The $\delta^{18}O_{cc}$ values were observed to decrease sharply (~−10.84‰) in Upper Eocene strata and increase gradually to intermediate and stable values in Lower Oligocene strata (~−9.45‰), followed by a decreasing trend up section (Fig. 2). The $\delta^{18}O$ values measured across growth lines of an oyster fossil yielded high variability along with growth increments (Fig. S4). The $\delta^{18}O$ and $\delta^{13}C$ values for shell, limestone, and adjacent continental red-bed samples were notably different (Fig. S4). In the western Tarim Basin, $\delta^{18}O_{cc}$ values from Upper Eocene nonmarine strata yielded a similar upward-decreasing trend as those from the Tajik Basin (Fig. 2).

The chemical proxy of alteration (CPA) in the Tajik Basin yielded the highest values (~90.01) in Upper Eocene strata, decreasing to low values (~80.35) in Lower Oligocene strata and returning to relatively high values (~84.44) in Upper Oligocene to Lower Miocene strata (Fig. 2; Table S2). X-ray diffraction (XRD) analyses indicated that clay minerals mainly comprise illite, smectite, and kaolinite (Figs. S5A and S5B). Scanning electron microscopy (SEM) data show that clay minerals in Upper Oligocene to Lower Miocene strata comprise a large portion of authigenic clays (Figs. S5C–S5F), such as honeycomb-shaped smectite, whereas those from Upper Eocene and Lower Oligocene strata are dominated by detrital clays (Figs. S5G–S5H).

Our climate simulations, using pre-industrial boundary conditions with a large areal extent of the Paratethys (Markwick, 2007; see Fig. S6 and Table S3), show an arid and semiarid climate over Central Asia (Fig. 3A). Modeled east-west climatological differences are present when relief of the Pamir–Tian Shan convergence zone is higher than 75% of modern elevation (~3000 m; Fig. 3B), whereas these differences disappear below 50% of modern elevations (~2000 m; Fig. 3C). Modeled seasonal precipitation patterns show that the regions west of the Pamir–Tian Shan have winter-spring precipitation maxima, whereas regions to the east have summer precipitation maxima (Fig. 3D). The west-east differences in precipitation seasonality become much weaker with progressively reducing topography in the Pamir–Tian Shan orogen (Figs. 3E and 3F). This is consistent with other simulations using a regional climate model (RegCM4.1, https://www.ictp.it/research/esp/models/regcm4.aspx) with late Oligocene boundary conditions (Liu et al., 2015).

DISCUSSION

Evaluating the $\delta^{18}O_{cc}$ Records

If continental sedimentary carbonates are formed early and under shallow burial conditions, the $\delta^{18}O$ values of these carbonates will reflect the isotopic composition and local temperature of surface waters (Quade and Roe, 1999). The following lines of evidence suggest that the $\delta^{18}O_{cc}$ values in this study are mainly related to syndepositional meteoric water or very early cementation. We observed distinctly different $\delta^{18}O$ and $\delta^{13}C$ values among shell, limestone, and adjacent continental red-bed samples (Fig. S4). This provides evidence that diagenesis has not reset the isotopic chemistry of the carbonates. Thin-section point counting of the sandstones suggests that a minor proportion (2.2%) of the total lithic grains in the samples are detrital carbonates (Table S4), and therefore they are

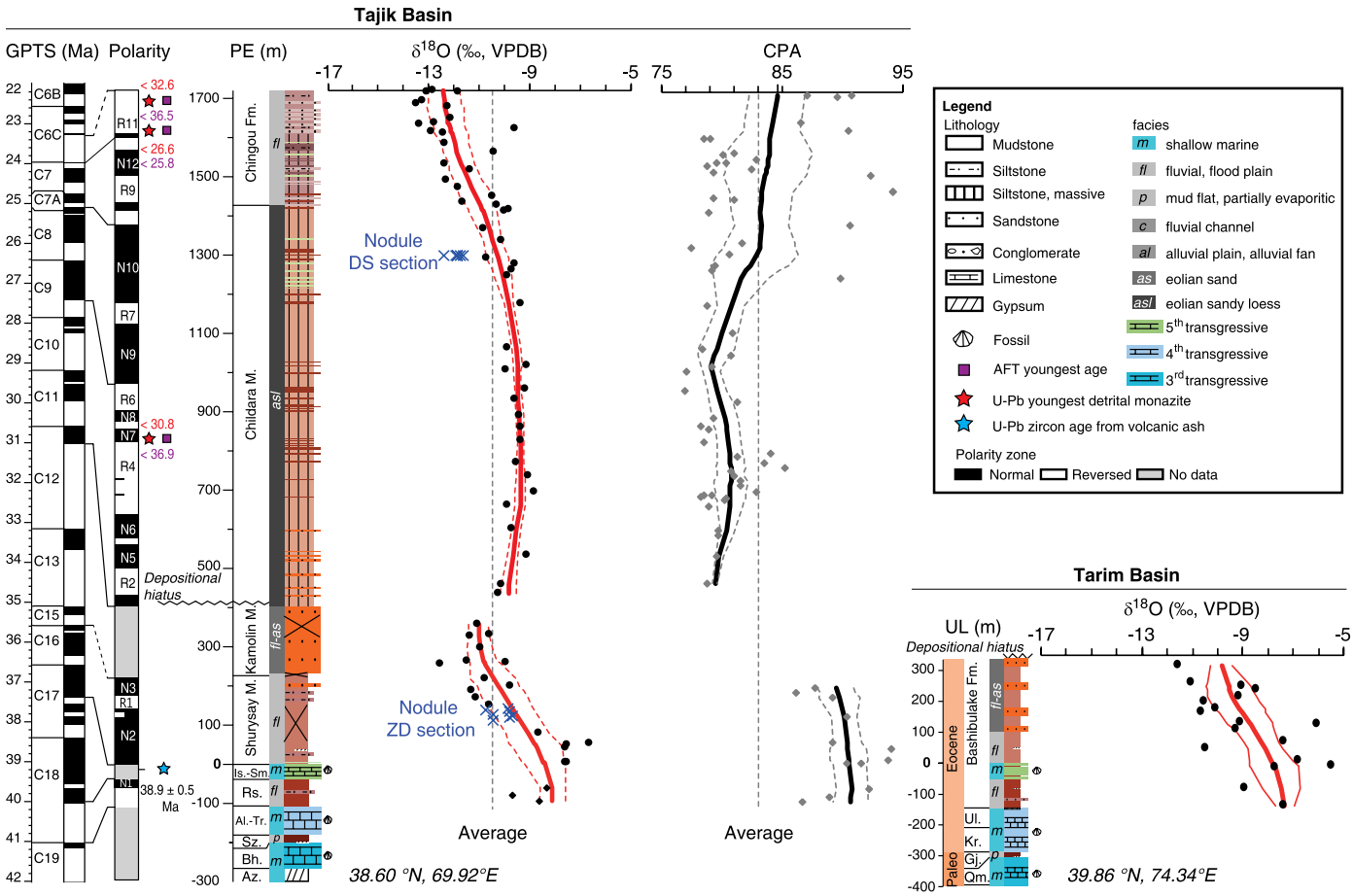

Figure 2. $\delta^{18}O_{cc}$ records of Lower Cenozoic sedimentary sequences in the Tajik and western Tarim basins. Chemical proxy of alteration (CPA) records from Tajik Basin and $\delta^{18}O$ values of carbonate nodules sampled from the ZD and DS sections are presented for comparison. Chronology is from Wang et al. (2019). Solid and dashed red lines are kernel-smoothing of data using Epanechnikov kernel (mean and 1σ) with 100 m bandwidth. Abbreviations: PE—Peshtova; ZD—Zidi; DS—Dashtijum; UL—Ulugqat; AFT—apatite fission track; GPTS—geomagnetic polarity time scale; Az.—Akdzha; Bh.—Bukhara; Sz.—Suzak; Al.—Alai; Tr.—Turkestan; Rs.—Rishtan; Is.—Isfara; Sm.—Sumsar; Shury.—Shurysay; M.—Member; Fm.—Formation; Qm.—Qimugen; Gj.—Gaijitage; Kr.—Karataer; Ul.—Ulagen; VPDB—Vienna Peedee belemnite.

unlikely to contaminate the stable isotopic data. High intergranular volume proportions (19%–40%; Table S4) suggest early sandstone cementation at shallow burial depth to prevent significant sandstone compaction (Zhuang et al., 2011). The $\delta^{18}O_{cc}$ values of Upper Eocene nonmarine strata are not identical (Fig. 2), suggesting that dissolved calcite from marine limestones, if any, had minimal impact on the $\delta^{18}O_{cc}$ compositions (Bershaw et al., 2012). Finally, the similarity between $\delta^{18}O$ values of carbonate cements and paleosol samples from an adjacent section (~60 km apart) in the Tajik Basin (Fig. 2) provides evidence that the cements were formed soon after deposition, and in environments very similar to the co-occurring soil carbonates.

Hydroclimate Differences Established in Central Asia since ca. 25 Ma

After the ultimate retreat of the Paratethys at ca. 37.4 Ma (Wang et al., 2019), an arid to semiarid climate regime was established in the Tajik Basin, as supported by the high $\delta^{13}C$ values of paleosols from the Dashtijum (DS) and Zidi (ZD) sections (Fig. S7) and the occurrence of eolian deposits in the Oligocene strata of the Peshtova (PE) section (Carrapa et al., 2015). The $\delta^{18}O_{cc}$ data from the Tajik Basin, the western Tarim Basin, and other sections from northwestern China (Kent-Corson et al., 2009) yielded comparable Paleogene decreasing trends (Fig. 4; Fig. S8), suggesting that there were no fundamental differences in the source of moisture between the windward and leeward sides of the Pamir–Tian Shan orogen, nor were there any high topographic barriers between the two regions during most of the Paleogene (Fig. S9). Paleogene $\delta^{18}O_{cc}$ decreasing trends likely were linked to the westward retreat of the Paratethys arising from the "continental effect" and/or due to late Eocene global cooling (Zachos et al., 2001), leading to lower $\delta^{18}O$ values of the regional rainfall (Hoefs, 2015).

The most significant changes in lithofacies and paleoclimate in the Tajik Basin occurred during the late Oligocene (ca. 25 Ma). Lithofacies in the Tajik Basin changed gradually from eolian sandy loess to fluvial-dominated facies (Fig. 2), consistent with a relatively wetter climate in the region after ca. 25 Ma (Wang et al., 2019). CPA values increase systematically starting in the late Oligocene (Fig. 2), suggesting enhanced chemical weathering and a relatively wetter climate (Ren et al., 2019) in the Tajik Basin and its catchments after ca. 25 Ma. SEM observations indicate that clay minerals in Lower Oligocene strata are dominated by detrital clays, whereas those in Upper Oligocene to Lower Miocene strata comprise a large portion of authigenic clays (Fig. S5), consistent with enhanced chemical weathering and poorly drained conditions (Wilson, 1999) in the Tajik Basin after ca. 25 Ma. These independent lines of evidence suggest a change in climate toward wetter conditions in the Tajik Basin after ca. 25 Ma, which is comparable to late Oligocene to early Miocene wetter climate changes in the Issyk Kul (Macaulay et al., 2016) and Ili basins (Hellwig et al., 2018) on the Tian Shan western flanks (Fig. 1A), but it is in contrast with the late Oligocene to early Miocene enhanced aridification in northwestern China and Mongolia on

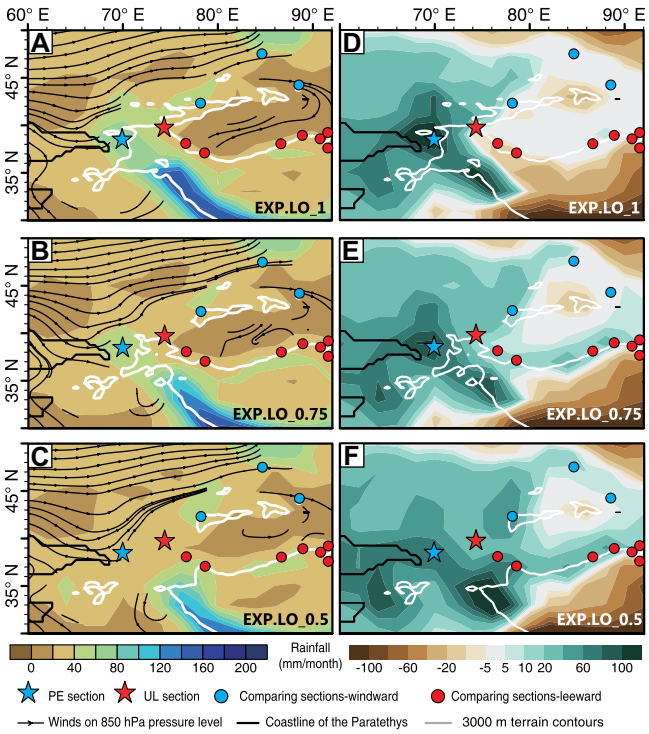

Figure 3. Climatic simulations: (A–C) precipitation annual amount and (D–F) seasonal precipitation differences between boreal winter and summer seasons simulated with high (~4000 m), medium (~3000 m), and low (~2000 m) mountains scenarios. Abbreviations for experimental names: EXP.LO—late Oligocene experiments, where 1, 0.75, 0.5 indicate 100%, 75%, and 50% of modern elevations of Pamir–Tian Shan convergence zone (34.5°N–43.5°N, 64°E–78°E), respectively.

the eastern side of the orogen (Guo et al., 2002; Zheng et al., 2015; Richoz et al., 2017).

Stable oxygen isotopic records from the windward and leeward sides of an orogen can be used to evaluate precipitation changes across topography and forcing mechanisms. The $\delta^{18}O_{cc}$ values decreased systematically in the Tajik Basin between ca. 25 and 23.3 Ma (Fig. 2). Comparison with the records from the Issyk Kul (Macaulay et al., 2016), Zaysan (Caves et al., 2017), and Junggar (Charreau et al., 2012) basins reveals that all of these basins that are windward or near-windward show decreasing $\delta^{18}O_{cc}$ starting in the late Oligocene (Fig. 4A). These decreasing $\delta^{18}O_{cc}$ trends contrast with nearly all $\delta^{18}O_{cc}$ records from northwestern China and Mongolia (Kent-Corson et al., 2009; Zhuang et al., 2011; Caves et al., 2014), on the leeward side of the orogen, which yield overall increasing trends since the late Oligocene (Fig. 4B).

Global temperature and ice-volume change no doubt played a role in driving regional climate changes, but these are unlikely to have been the main contributor for the establishment of the west-east hydroclimate differences over Central Asia (Fig. 4), as these factors would have affected the two regions similarly. Instead, we posit that significant topography associated with the Pamir–Tian Shan orogen best explains the opposite trends in $\delta^{18}O_{cc}$ records between the windward and leeward sides of the orogen since the late Oligocene. First, a wetter climate, associated with increased orographic precipitation on the windward side of the mountains (Figs. 3A–3C), can explain a decrease in $\delta^{18}O_{cc}$, consistent with increased humidity and lower postcondensation evaporation (Hoefs, 2015). Second, an increase in the elevation of the study region's catchments could shift the basinal $\delta^{18}O_{cc}$ to lower values, as authigenic carbonates recorded high-elevation waters from the growing Pamirs to the south (Wang et al., 2019). Third, a change in precipitation seasonality toward dominant winter precipitation may have influenced the timing of pedogenic carbonate formation, thereby decreasing $\delta^{18}O_{cc}$ values due to lower $\delta^{18}O$ values of precipitation in the winter (Caves et al., 2017). The overall increasing $\delta^{18}O_{cc}$ values during the Neogene in records from northwestern China and Mongolia on the leeward (east) side of the Pamir and Tian Shan are broadly interpreted as a result of enhanced aridification (Zhuang et al., 2011). All these mechanisms require the establishment of a modern-like tectonic-climatic configuration during the late Oligocene (Fig. 1B).

When integrated with geological evidence, our new data suggest that a significant part of the Pamir–Tian Shan mountains had reached elevations of ~3 km and acted as a moisture barrier for the westerlies since ca. 25 Ma. Interestingly, in our simulations, monsoon precipitation in the Himalaya also decreases when the Pamir–Tian Shan convergence zone is lowered (Figs. 3B and 3C), suggesting a possible control by Pamir–Tian Shan topography on westerlies and the Asian monsoon.

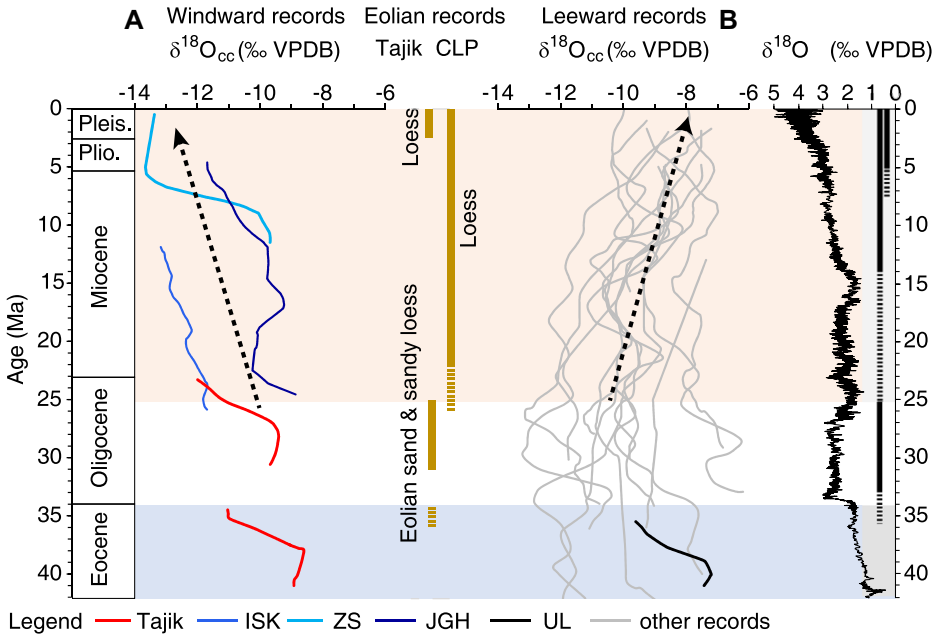

Figure 4. $\delta^{18}O_{cc}$ data from the Tajik Basin and other published data from Central Asia (see text for citations), and comparison with benthic oxygen isotope stack curve (Zachos et al., 2001). All data were smoothed using 1 m.y. bandwidth Epanechnikov kernel. Eolian records were used as proxy for productive ability of silt-sized materials, which is expected to be higher under a drier climate with low vegetation cover in source regions (Zheng et al., 2015). ISK—Issyk Kul (Macaulay et al., 2016); ZS—Zysan (Caves et al., 2017); UL—Ulugqat (Wang et al., 2014); JGH—Jingouhe (Charreau et al., 2012); CLP—Chinese Loess Plateau; Plio.—Pliocene; Pleis.—Pleistocene; VPDB—Vienna Peedee belemnite.

ACKNOWLEDGMENTS

We thank Huayu Lu, John Bershaw, and anonymous reviewers for their constructive comments. This work is supported by the National Natural Science Foundation of China (grant 41672158), the second Tibetan

Plateau Scientific Expedition and Research Program (grant 2019QZKK0602), the U.S. National Science Foundation (grant EAR-1450917), and the Helmholtz Postdoc Program (grant PD-301).

REFERENCES CITED

An, Z.S., 2014, Late Cenozoic Climate Change in Asia: Dordrecht, Netherlands, Springer, 587 p., https://doi.org/10.1007/978-94-007-7817-7.

Baldwin, J., and Vecchi, G., 2016, Influence of the Tian Shan on arid extratropical Asia: Journal of Climate, v. 29, p. 5741–5762, https://doi.org/10.1175/JCLI-D-15-0490.1.

Bande, A., Sobel, E.R., Mikolaichuk, A., Schmidt, A., and Stockli, D.F., 2017, Exhumation history of the western Kyrgyz Tien Shan: Implications for intramontane basin formation: Tectonics, v. 36, p. 163–180, https://doi.org/10.1002/2016TC004284.

Bershaw, J., Garzione, C. N., Schoenbohm, L., Gehrels, G., and Tao, L., 2012, Cenozoic evolution of the Pamir plateau based on stratigraphy, zircon provenance, and stable isotopes of foreland basin sediments at Oytag (Wuyitake) in the Tarim Basin (west China): Journal of Asian Earth Science, v. 44, p. 136–148, https://doi.org/10.1016/j.jseaes.2011.04.020.

Blayney, T., Dupont-Nivet, G., Najman, Y., Proust, J.-N., Meijer, N., Roperch, P., Sobel, E.R., Millar, I., and Guo, Z., 2019, Tectonic evolution of the Pamir recorded in the western Tarim Basin (China): Sedimentologic and magnetostratigraphic analyses of the Aertashi section: Tectonics, v. 38, p. 492–515, https://doi.org/10.1029/2018TC005146.

Carrapa, B., DeCelles, P.G., Wang, X., Clementz, M.T., Mancin, N., Stoica, M., Kraatz, B., Meng, J., Abdulov, S., and Chen, F.H., 2015, Tectonoclimatic implications of Eocene Paratethys regression in the Tajik Basin of Central Asia: Earth and Planetary Science Letters, v. 424, p. 168–178, https://doi.org/10.1016/j.epsl.2015.05.034.

Caves, J.K., Sjostrom, D.J., Mix, H.T., Winnick, M.J., and Chamberlain, C.P., 2014, Aridification of Central Asia and uplift of the Altai and Hangay Mountains, Mongolia: Stable isotope evidence: American Journal of Science, v. 314, p. 1171–1201, https://doi.org/10.2475/08.2014.01.

Caves, J.K., Winnick, M.J., Graham, S.A., Sjostrom, D.J., Mulch, A., and Chamberlain, C.P., 2015, Role of the westerlies in Central Asia climate over the Cenozoic: Earth and Planetary Science Letters, v. 428, p. 33–43, https://doi.org/10.1016/j.epsl.2015.07.023.

Caves, J.K., Bayshashov, B.U., Zhamangara, A., Ritch, A.J., Ibarra, D.E., Sjostrom, D.J., Mix, H.T., Winnick, M.J., and Chamberlain, C.P., 2017, Late Miocene uplift of the Tian Shan and Altai and reorganization of Central Asia climate: GSA Today, v. 27, no. 2, p. 19–26, https://doi.org/10.1130/GSATG305A.1.

Chapman, J.B., Carrapa, B., DeCelles, P.G., Worthington, J., Mancin, N., Cobianchi, M., Stoica, M., Wang, X., Gadoev, M., and Oimahmadov, I., 2019, The Tajik Basin: A composite record of sedimentary basin evolution in response to tectonics in the Pamir: Basin Research, https://doi.org/10.1111/bre.12381 (in press).

Charreau, J., Kent-Corson, M.L., Barrrier, L., Augier, R., Ritts, B.D., Chen, Y., France-Lannord, C., and Guilmette, C., 2012, A high-resolution stable isotopic record from the Junggar Basin (NW China): Implications for the paleotopographic evolution of the Tianshan Mountains: Earth and Planetary Science Letters, v. 341–344, p. 158–169, https://doi.org/10.1016/j.epsl.2012.05.033.

Chen, F.H., et al., 2019, Westerlies Asia and monsoonal Asia: Spatiotemporal differences in climate change and possible mechanisms on decadal to sub-orbital timescales: Earth-Science Reviews, v. 192, p. 337–354, https://doi.org/10.1016/j.earscirev.2019.03.005.

Guo, Z.T., Ruddiman, W.F., Hao, Q.Z., Wu, H.B., Qiao, Y.S., Zhu, R.X., Peng, S.Z., Wei, J.J., Yuan, B.Y., and Liu, T.S., 2002, Onset of Asian desertification by 22 Myr ago inferred from loess deposits in China: Nature, v. 416, p. 159–163, https://doi.org/10.1038/416159a.

Heermance, R.V., Pearson, J., Moe, A., Liu, L.T., Xu, J.H., Chen, J., Richter, F., Garzione, C.N., Nie, J.S., and Bogue, S., 2018, Erg deposition and development of the ancestral Taklimakan Desert (western China) between 12.2 and 7.0 Ma: Geology, v. 46, p. 919–922, https://doi.org/10.1130/G45085.1.

Hellwig, A., Voigt, S., Mulch, A., Frisch, K., Bartenstein, A., Pross, J., Gerdes, A., and Voigt, T., 2018, Late Oligocene to early Miocene humidity change recorded in terrestrial sequences in the Ili Basin (south-eastern Kazakhstan, Central Asia): Sedimentology, v. 65, p. 517–539, https://doi.org/10.1111/sed.12390.

Hoefs, J., 2015, Stable Isotope Geochemistry: Geneva, Switzerland, Springer, 389 p., https://doi.org/10.1007/978-3-319-19716-6 .

Jepson, G., Glorie, S., Konopelko, D., Gillespie, J., Daniš́k, M., Evans, N.J., Mamadjanov, Y., and Collins, A.S., 2018, Thermochronological insights into the structural contact between the Tian Shan and Pamirs, Tajikistan: Terra Nova, v. 30, p. 95–104, https://doi.org/10.1111/ter.12313.

Kalnay, E., et al., 1996, The NCEP/NCAR 40-year reanalysis project: Bulletin of the American Meteorological Society, v. 77, p. 437–471, https://doi.org/10.1175/1520-0477(1996)077<0437:TNYRP>2.0.CO;2.

Kent-Corson, M.L., Ritts, B.D., Zhuang, G., Bovet, P.M., Graham, S.A., and Page Chamberlain, C., 2009, Stable isotopic constraints on the tectonic, topographic, and climatic evolution of the northern margin of the Tibetan Plateau: Earth and Planetary Science Letters, v. 282, p. 158–166, https://doi.org/10.1016/j.epsl.2009.03.011.

Liu, X.D., Sun, H., Miao, Y.F., Dong, B.W., and Yin, Z.Y., 2015, Impacts of uplift of northern Tibetan Plateau and formation of Asian inland deserts on regional climate and environment: Quaternary Science Reviews, v. 116, p. 1–14, https://doi.org/10.1016/j.quascirev.2015.03.010.

Lu, H.Y., Wang, X.Y., and Li, L.P., 2010, Aeolian sediment evidence that global cooling has driven late Cenozoic stepwise aridification in Central Asia, *in* Clift, P.D., et al., eds., Monsoon Evolution and Tectonics–Climate Linkage in Asia: Geological Society [London] Special Publication 342, p. 29–44, https://doi.org/10.1144/SP342.4.

Macaulay, E.A., Sobel, E.R., Mikolaichuk, A., Wack, M., Gilder, S.A., Mulch, A., Fortuna, A.B., Hynek, S., and Apayarov, F., 2016, The sedimentary record of the Issyk Kul basin, Kyrgyzstan: Climatic and tectonic inferences: Basin Research, v. 28, p. 57–80, https://doi.org/10.1111/bre.12098.

Markwick, P.J., 2007, The palaeogeographic and palaeoclimatic significance of climate proxies for data-model comparisons, *in* Williams, M., et al., eds., Deep-Time Perspectives on Climate Change: Marrying the Signal from Computer Models and Biological Proxies: The Micropalaeontological Society Special Publication 2, Geological Society [London], p. 251–312, https://doi.org/10.1144/TMS002.13.

Quade, J., and Roe, L.J., 1999, The stable-isotope composition of early ground-water cements from sandstone in paleoecological reconstruction: Journal of Sedimentary Research, v. 69, p. 667–674, https://doi.org/10.2110/jsr.69.667.

Ramstein, G., Fluteau, F., Besse, J., and Joussaume, S., 1997, Effect of orogeny, plate motion and land-sea distribution on Eurasian climate change over the past 30 million years: Nature, v. 386, p. 788–795, https://doi.org/10.1038/386788a0.

Ren, X., Nie, J., Saylor, J.E., Li, H., Bush, M.A., and Horton, B.K., 2019, Provenance control on chemical weathering index of fluvio-lacustrine sediments: Evidence from the Qaidam Basin, NE Tibetan Plateau: Geochemistry Geophysics Geosystems, v. 20, p. 3216–3224, https://doi.org/10.1029/2019GC008330.

Richoz, S., Baldermann, A., Frauwallner, A., Harzhauser, M., Daxner-Höck, G., Klammer, D., and Piller, W.E., 2017, Geochemistry and mineralogy of the Oligo-Miocene sediments of the Valley of Lakes, Mongolia: Palaeobiodiversity and Palaeoenvironments, v. 97, p. 233–258, https://doi.org/10.1007/s12549-016-0268-6.

Sobel, E.R., and Dumitru, T.A., 1997, Thrusting and exhumation around the margins of the western Tarim Basin during the India-Asia collision: Journal of Geophysical Research, v. 102, no. B3, p. 5043–5063, https://doi.org/10.1029/96JB03267.

Stepanek, C., and Lohmann, G., 2012, Modelling mid-Pliocene climate with COSMOS: Geoscientific Model Development, v. 5, p. 1221–1243, https://doi.org/10.5194/gmd-5-1221-2012.

Wang, X., Sun, D.H., Chen, F.H., Wang, F., Li, B.F., Popov, S.V., Wu, S., Zhang, Y.B., and Li, Z.J., 2014, Cenozoic paleo-environmental evolution of the Pamir–Tien Shan convergence zone: Journal of Asian Earth Sciences, v. 80, p. 84–100, https://doi.org/10.1016/j.jseaes.2013.10.027.

Wang, X., et al., 2019, Paratethys last gasp in Central Asia and late Oligocene accelerated uplift of the Pamirs: Geophysical Research Letters, v. 46, p. 11773–11781, https://doi.org/10.1029/2019GL084838.

Wilson, M.J., 1999, The origin and formation of clay minerals in soils: Past, present and future perspectives: Clay Minerals, v. 34, p. 7–25, https://doi.org/10.1180/000985599545957.

Zachos, J., Pagani, M., Sloan, L., Thomas, E., and Billups, K., 2001, Trends, rhythms, and aberrations in global climate 65 Ma to present: Science, v. 292, p. 686–693, https://doi.org/10.1126/science.1059412.

Zheng, H.B., Wei, X.C., Tada, R., Clift, P.D., Wang, B., Jourdan, F., Wang, P., and He, M.Y., 2015, Late Oligocene–early Miocene birth of the Taklimakan Desert: Proceedings of the National Academy of Sciences of the United States of America, v. 112, p. 7662–7667, https://doi.org/10.1073/pnas.1424487112.

Zhuang, G.S., Hourigan, J.K., Koch, P.L., Ritts, B.D., and Kent-Corson, M.L., 2011, Isotopic constraints on intensified aridity in Central Asia around 12 Ma: Earth and Planetary Science Letters, v. 312, p. 152–163, https://doi.org/10.1016/j.epsl.2011.10.005.

Printed in USA